

Synthesis and Characterization of PtRuMo/C Ternary Nanoelectrocatalysts for Direct Methanol Fuel Cells

Van Thi Thanh Ho^{1*}, Long Giang Bach²

¹Hochiminh City University of Natural Resources and Environment, Vietnam

²NTT Institute of High Technology, Nguyen Tat Thanh University, Ho Chi Minh City, Vietnam

Abstract—Direct methanol fuel cells (DMFCs) are the most promising power source for portable and small devices because of their advantages of high energy density, low pollutant emission, low operating temperature, and ease of handling liquid fuel. However, there are some problems in the commercialization of DMFCs. Most commonly used Pt catalyst shows slow kinetics for methanol electro-oxidation, which is caused by self-poisoning of Pt catalyst surface and the high cost of PtRu novel metal on carbon. Herein, the ternary electrocatalysts based on carbon supported PtRuMo/C nanoparticles are prepared by chemical reduction method in this work. The crystallographic properties, morphology and composition of the catalysts are characterized by X-ray diffraction (XRD), transmission electron microscopy (TEM) and energy dispersive X-ray (EDX), and the catalytic performance for methanol electro-oxidation was measured by cyclic voltammetry (CV). The catalytic activity and stability of the PtRuMo/C catalyst are determined and compared with the catalyst of Pt/C nanoparticles prepared by the same method.

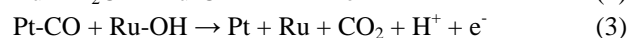
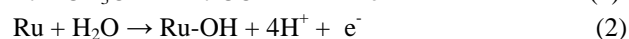
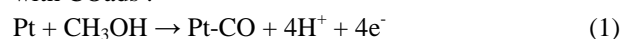
Keywords— DMFC, PtRuMo/C, CO poisoning, fuel cells, ternary electrocatalysts.

I. INTRODUCTION

In the recently, the direct methanol fuel cell (DMFC) has been considered as a highly promising power source because it possess a number of advantages such as a liquid fuel, quick refueling, low cost of methanol, design making it suitable for various potential applications including stationary and portable applications [1-4]. Therefore, intensive research on the DMFC has been carried out. Although a significant progress has been made in this field[5,6,7], its performance is still limited by the slow electro-oxidation kinetics, the methanol crossover from anode side to cathode through polymer proton exchange membrane[7,8] and CO tolerance[5-9]. In order to solve these problems, many studies recently have been focused on the development of highly active

catalysts for methanol electro-oxidation reaction (MOR)[5-10].

At present, Pt metal and Pt-Ru alloy are usually used as anode and cathode catalysts for DMFC, respectively. In the PtRu alloy catalyst, Ru plays an important role to improve CO tolerance property of pure Pt[11,12]. The pure Pt catalyst shows high activity for the MOR, but a rapid drop of activity is followed because of poisoning by adsorbed CO (COads) which is an intermediate of the MOR. Under the “bi-functional mechanism” as shown below, Ru dissociates water to produce Ru-OH to react with COads :



Although the PtRu catalysts exhibit much higher MOR activity than that of pure Pt[11-14], the cost of the catalysts is still expensive for both Pt and Ru are the noble metal. Thus, researchers should search for ways to minimize or eliminate the usage of this precious metal in catalysts. In the recent review, various Pt-Ru based ternary catalysts have been introduced as promising MOR catalysts such as: PtRuCu, PtRuNi, PtRuCo and so on[15,16]. In this study, we selected Mo as third component. The addition of a third metal is one of the obvious choices for maintaining the performance of the electrode and lowering of the electrode and lowering the usage of Pt and Ru in the catalyst. Molybdenum is an inexpensive and amply available metal element. Recently, both experimental and theoretical investigations have indicated that PtMo alloy could be a better catalyst for oxidation than PtRu. As compared with the extensive studies on the carbon supported PtMo alloy anodic catalysts in DMFC [17,18,19]. In our previous work, we presented a new approach by exploring robust noncarbon. $\text{Ti}_{0.7}\text{Mo}_{0.3}\text{O}_2$ used as a novel functionalized cocatalytic support for Pt. This study is based on the novel nanostructure $\text{Ti}_{0.7}\text{Mo}_{0.3}\text{O}_2$ support with “electronic transfer mechanism” from $\text{Ti}_{0.7}\text{Mo}_{0.3}\text{O}_2$ to Pt [20].

As noted above, Mo was chosen as a third member of the PtRu catalyst to improve the performance and increase the cost of DMFC. In this study, the ternary electrocatalysts based on carbon supported PtRuMo/C nanoparticles was prepared by chemical reduction method and the results were compared to those with the catalyst of PtRu/C prepared by the same method. The crystallographic properties, morphology and composition of the catalysts are characterized by X-ray diffraction (XRD), transmission electron microscopy (TEM) and the catalytic performance for methanol electro-oxidation was measured by cyclic voltammetry (CV).

II. EXPERIMENT

1. Materials

Vulcan XC-72R carbon with particles size ~ 60 nm using as a support was purchased from Fuel Cell Store (USA). All the chemicals were of analytical grade; Hydrogen hexachloroplatinate (VI) ($\text{H}_2\text{PtCl}_6 \cdot 6\text{H}_2\text{O}$), Ruthenium(III) chloride hydrate ($\text{RuCl}_3 \cdot x\text{H}_2\text{O}$), Ammonium molybdate tetrahydrate ($(\text{NH}_4)_6\text{Mo}_7\text{O}_{24} \cdot 4\text{H}_2\text{O}$), Methyl alcohol pure (CH_3OH) (Acros). Sodium borohydride (NaBH_4), Nitric acid (HNO_3 , 65-68%), Sulfuric acid (H_2SO_4 , 95-98%), Iso propyl alcohol (China) were used.

2. Preparation of pre-treated Vulcan XC-72R

Vulcan XC-72R carbon powder was treated to clean the contaminant in the commercial carbon. For example, 0.5g Carbon was dispersed in a round bottom flask with 500 ml of the 5% HNO_3 solution, the mixture was refluxed for 16 hours at 110°C . Treated carbon were centrifuged with 4000rpm until no H^+ and NO_3^- with the pure water and acetone, then dried at 105°C in an oven for 10 hours.

3. Preparation of PtRuMo/C nanoparticles catalysts with different ratio (3:1:1), (2:1:1) and (3:2:1)

At first, the carbon black was dispersed into a mixture of pure water and isopropyl alcohol through 20 min of ultrasonication to make a uniform carbon ink. Then, the precursors were added to the ink ultrasonically for 20 min. The pH value of the mixture was adjusted by NaOH solution to 9 and then its temperature was increased to 80°C immediately before the drop-by-drop addition of 25ml of 0.2 mol L^{-1} solution of sodium borohydride, which was followed by stirring the bath for 1 hour. The product was cooled, dried and washed by repeatedly with ultra-pure water until Na^+ and $\text{B}(\text{OH})_4^-$ ions were detected. The formed powder of catalyst was dried for 3h at 100°C and then stored in a vacuum vessel.

4. Preparation of working electrode and Electrochemical measurements.

Using a pipette for spread the ultrasonically re-dispersed catalyst suspension ($5\mu\text{l}$) onto the glassy carbon substrate.

After the solvent evaporation, the deposited catalyst ($28 \mu\text{g metal cm}^{-2}$) was covered with $5\mu\text{l}$ of a dilute aqueous Nafion solution. The resulting Nafion film layer with a thickness less than $0.2\mu\text{m}$ had the sufficient strength to keep carbon working electrode without producing significant diffusion resistances. Finally, a glassy carbon working electrode was made with a diameter of 3mm and an electrode area of 0.0706 cm^2 was polished with $0.05\mu\text{m}$ alumina to a mirror finish before each experiment, were used as substrates for the Vulcan-supported catalysts.

All measurements were carried out in the conventional three-electrode electrochemical cell at 25°C , in which the glassy carbon electrode made in the above mentioned procedure served as the working electrode and a piece of Pt foil (1cm^2) as the counter electrode and a saturated calomel electrode were used as reference electrode. All solutions were prepared with the chemicals of analytical grade and the ultra-pure water. The ultra-pure nitrogen gas was utilized to continuously purge the solution system of $0.5 \text{ mol L}^{-1} \text{ H}_2\text{SO}_4$, which was kept under constantly stirring state. The cyclic voltammograms (CV) were plotted within a potential range from 0.05 to 1.2V at scanning rate of 0.05Vs^{-1}

5. Characterization

X-ray powder diffraction (XRD) patterns were recorded by using a Cu $\text{K}\alpha$ radiation source on a D8 Advance Bruker powder diffractometer (University of Technology – VNU HCM City). Transmission electron microscope (TEM) was taken by JEM -1400 (JEOL, Japan), (University of Technology-VNU HCM City). Cyclic Voltammetry (CV) was recorded by AutoLab machine system at Applied Physical Laboratory, University of Science, VNU-HCM, Vietnam.

III. RESULT AND DISCUSSION

1. XRD characterization

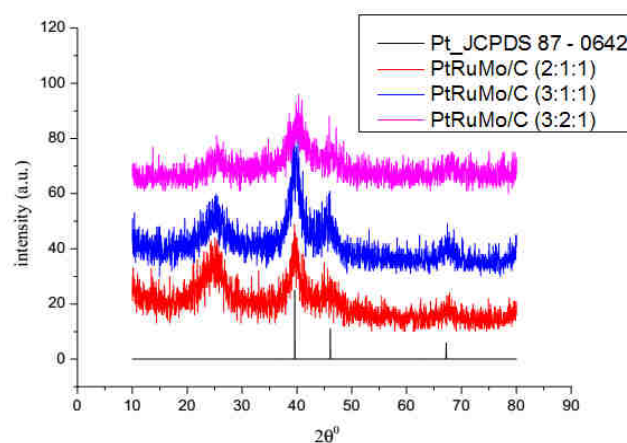


Fig.1: X-ray powder diffraction of PtRuMo/C catalysts

X-ray diffraction of these samples is shown in the Fig. 1. It indicates that all the broad diffraction peaks of the XRD patterns at $2\theta = 39.6, 47.4, 67.1^\circ$, corresponding to the reflections (111), (200), (220), respectively, which are consistent with the face centered cubic (fcc) structure of platinum, can be assigned to (JCPDS Card 04 -0802), thus demonstrating the presence of crystalline Pt [21]. In addition, a broad peak at $2\theta \approx 25^\circ$ was observed but not clearly due to the (002) plane of the hexagonal structure of the carbon support (Vulcan XC-72R) is amorphous carbon with small regions of graphitic properties [21]. These patterns indicate the domain feature of the disordered single-phase structures for the ternary. The lack of characteristic peaks of Ru, Mo and their oxides/hydroxides suggests the possibility that Ru and Mo atoms or exist as oxides in amorphous phase. The average particle sizes and specific surface areas, which are estimated from full width at half maximum (FWHM) according to Debye-Scherrer formula [22,23] as follows:

$$\rho_{Pt-Ru-Ni} = X_{Pt} \times \rho_{Pt} + X_{Ru} \times \rho_{Ru} + X_{Mo} \times \rho_{Mo}$$

$$d = \frac{k\lambda}{\beta_{1/2} \cos\theta}$$

$$S = \frac{60,000}{\rho d}$$

Where d is the average particle sizes (A^0), θ the angle, at which the peak maximum occurs, $\beta_{1/2}$ the width (in radians) of the diffraction peak at a half height, λ the wave length of X-ray ($1.5406 A^0$), k is a coefficient of 0.89 to 1.39 (0.9 here), ρ is the density of PtRuMo ternary particles: ρ_{Ru} the density of Ru metal (12.45 gcm^{-3}), ρ_{Pt} is the density of Pt metal (21.45 gcm^{-3}), ρ_{Mo} is the density of Mo metal (10.3 gcm^{-3}), and X_{Pt} , X_{Ru} , X_{Mo} are the weight percent of Pt, Ru and Mo, respectively, in the catalysts. After calculated, the average particle sizes and specific surface areas of nanoparticle catalysts are presented in Table 1.

Table 1. The particle size and specific area of the PtRuMo/C nanoparticle electrocatalysts

Samples	Average particle size (nm)	Specific surface areas (m^2g^{-1})
PtRuMo/C (3:1:1)	4.22	81.6
PtRuMo/C (2:1:1)	4.9	74.6
PtRuMo/C (3:2:1)	5.26	68.75

2. TEM measurement

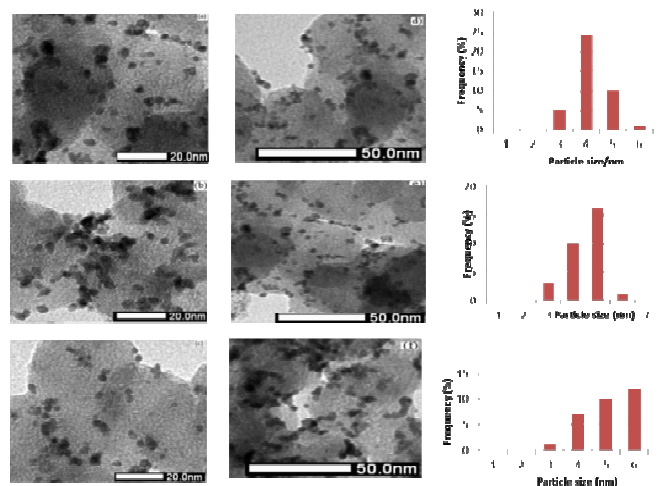


Fig.2:TEM imag of nanoparticles catalysts: a),d) PtRuMo/C(3:1:1), b),e) PtRuMo/C(2:1:1), c),e) PtRuMo/C (3:2:1)

Figure 2 shows TEM micrographs of PtRuMo/C nanoparticle catalysts. The dark black portions are Pt grains, and the grey portions are carbon support grains. It is clearly shown that the spherical metal particles spread homogeneously on carbon support grains in both catalyst systems and the average of particles sizes range from 3 to 6 nm, close to the calculated XRD values.

3. Cyclic Voltammetry (CV) results

Figure 3 shows CV curves of Pt/C catalysts in H_2SO_4 0.5M solution. From the CV curves, it was easy to calculate the charge of the electrochemical processes which occur on the catalyst particles by integrating. As a result, the electrochemical surface area (ESA) showing the activity of the catalysts was estimated by the following formula [24,25]:

$$S_{ESA-H} = \frac{Q_H}{[Pt] \times Q_{monolayer}} = \frac{1}{v} \times \frac{\int i(E)dE}{[Pt] \times 2,1}$$

Where, S_{ESA-H} is electrochemically active surface area (m^2/gPt), Q_H is the charge for hydrogen desorption (C or A.s), $\int i(E)dE$ is integral of part hydrogen desorption (A.V), 2,1 is $Q_{monolayer}$ (C.cm^{-2}) (the charge related to the adsorption or desorption of a hydrogen monolayer on a polycrystalline Pt surface), v is scan rate (mV.s^{-1}) and $[PtRuMo]$ represents the catalysts loading in the electrode (g). The result of ESA values are listed in Table 2.

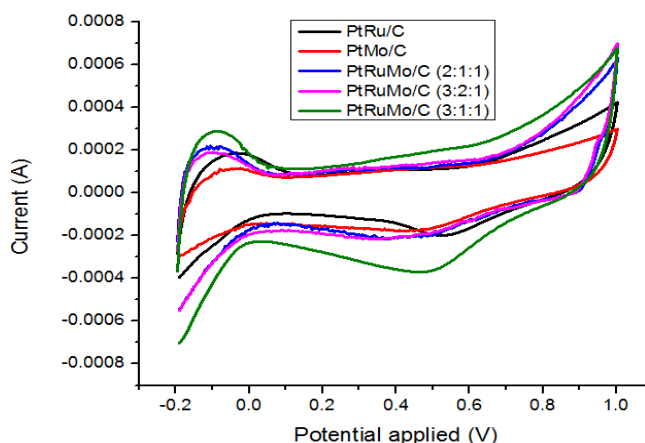


Fig.3: Cyclic voltammograms in a N_2 -saturated solution of $0.5 \text{ mol L}^{-1} \text{ H}_2\text{SO}_4$ at 25°C on the PtMo/C, PtRu/C and PtRuMo/C nanoparticles. Scanrate rate: 0.02 V s^{-1}

Table 2. The electrochemically active surface area (SESA-H) of PtRuMo/C nanoparticles catalysts.

Samples	$S_{(\text{ESA-H})}(\text{m}^2/\text{g})$
PtMo/C (3:1)	9.95
PtRu/C (3:1)	34.79
PtRuMo/C (3:2:1)	37.6
PtRuMo/C (2:1:1)	41.4
PtRuMo/C (3:1:1)	55.69

On the CV curves (Fig. 3), there are the electrochemical peaks corresponding to the different electrochemical reactions on the samples' surface. In the potential range about $-0.15 - 0.15 \text{ V}$, the peaks express the adsorption/desorption processes of hydrogen on Pt, Ru and Mo crystal. The mechanism of these processes may take place by two stages. In the forward scan, the potential range from 0.15 to 0.58 V corresponds to the charge of the double layer by the oxygenated groups on the carbon support surface. At the potential 0.65 V , the oxidation process of Pt, Ru, Mo metal happens to form oxides corresponding. Among the peaks of the catalyst samples, The activity of the PtRuMo/C (3:1:1) is the highest ($55.69 \text{ m}^2/\text{g}$). The calculated ESA values of the catalyst samples are shown in table 2. The difference in ESA value may be due to the role of Ru, Mo in catalyst samples. With the atom ratio of Pt:Mo(3:1) not Ru, the ESA value of the PtMo/C (3:1) sample is the smallest ($9.95 \text{ m}^2/\text{g}$) corresponding to desorption peak lowest. These results provide an extremely significant information about the role of Ru and Mo and activity of the PtRuMo/C nanoparticles catalyst on carbon support: The catalysts with smaller particle size will give a higher activity due to larger surface area. This trend also corresponds with the results of TEM and XRD analysis.

IV. CONCLUSION

The PtRuMo/C nanoparticle catalyst with different ratio, formed through the reduction of inorganic precursor salts with NABH_4 , is superior to the similarly synthesized Pt/C nanoparticle catalyst. The activity of the PtRuMo/C (3:1:1) is the highest ($55.69 \text{ m}^2/\text{g}$). This means that the PtRuMo/C ternary catalyst help solving the problem of the anode poisoning in DMFC and increase the cost of DMFC.

ACKNOWLEDGEMENTS

This work was supported by Ho Chi Minh City University of Technology, University Of Science Ho Chi Minh City, Ho Chi Minh City University of Natural Resources and Environment.

REFERENCES

- [1] S. Sun, G. Zhang, Y. Zhong, H. Liu, R. Li, X. Zhou and X. Sun, Chemical Communications pp. 7048-7050, 2009.
- [2] B.Y. Xia, H.B. Wu, Y. Yan, X. Wen, and X. Wang, J. Am. Chem. Soc. Vol. 135, no. 25, pp 9480-9485, 2013.
- [3] Y. Lu, S. Du, R. Steinberger-Wilckens, Applied Catalysis B: Environmental, vol. 164, pp. 389-395, 2015.
- [4] Thesis Alexandere Hacquard, Chemical Engineering, 5(2005)
- [5] R.N. Singh, R. Awasthi and C.S. Sharma, Electrochimica Acta, 2014, 5067-5639.
- [6] Hamnett, Catalysts Today vol. 38, pp. 445-457, 1997.
- [7] Z.C. Tang, G.X. Lu, Applied Catalysis B: Environmental, vol. 1, pp. 1-7, 2008.
- [8] R.Z. Jiang, C. Rong, D. Chu, J. Power Sources 126 (1-2) (2004) 119
- [9] W. Vielstich, A. Lamm, H.A. Gasteiger, Handbook off Fuel Cells: Fundamentals Technology and Applications; Wiley: West Sussex, U.K, 2003.
- [10] T. Ghosh, M.B. Vukmirovic, F.J. DiSalvo; R.R. Adzic, Journal of the American Chemical Society, vol. 132, pp. 906-907, 2010.
- [11] T.C. Deivaraj, J.Y. Lee, Journal of Power Sources, vol. 142, pp. 43-49, 2005.
- [12] T. Seiler, E.R. Savinova, K.A. Friedrich, U. Stimming, Electrochimica Acta, vol. 49, pp. 3927-3936, 2004.
- [13] H.A. Gasteiger, P.N. Ross, E.J. Cairns, Journal of The Electrochemical Society, vol. 141, pp. 1795-1803, 1994.
- [14] F. Vigier, C. Coutanceau, A. Perrard, E.M. Belgsir, C. Lamy, Journal of Applied Electrochemistry, vol. 34, pp. 17-23, 2004.

- [15] T.C. Deivaraj, J.Y. Lee, Journal of Power Sources, vol. 142, pp. 43-49, 2005.
- [16] M.K. Jeon, J.S. Cooper, P.J. McGinn, Journal of Power Sources, vol 185, pp. 913-916, 2008.
- [17] B.N. Grgur, N.M. Markovic, Journal of Physical Chemistry B, vol. 102, pp. 2494-2501, 1998.
- [18] S. Mukerjee, S.J. Lee, E.A. Ticianelli, J.B. McBreen, N. Grgur, N.M. Markovic, P.N. Ross, J.R. Giallombardo, E.S. de Castro, Electrochem. Solid-State Letter vol. 2, pp. 12-15, 1999
- [19] E.I. Santiago, G.A. Camara, E.A. Ticianelli, Electrochimica Acta, vol. 48, pp. 3527-3534, 2003.
- [20] V.T.T. Ho, C.J. Pan, J. Rick, W.N. Su, B.J. Hwang, Journal of the American Chemical Society, vol. 133, pp. 11716-11724, 2011.
- [21] C.Z. He, H.R. Kunz, J.M. Fenton, Journal of The Electrochemical Society, vol. 144, pp. 970-979, 1997.
- [22] Z.B. Wang, G.P. Yin, P.F. Shi, Journal of The Electrochemical Society, vol. 152, pp. A2406-A2412, 2005.
- [23] W. Wang, M. Zhu, X. Lu, Y. Gao, L. Li, Z. Cao, C. Li, J.Liu, H. Zheng, Journal Name. vol. 00, pp. 1-3, 2013.
- [24] A. Pozio, M. De Francesco, A. Cemmi, F. Cardellini, L. Giorgi. Journal of Power Sources, vol. 105, pp. 13-19, 2002.
- [25] J. Perez, E.R. Gonzalez, E.A. Ticianelli, Electrochimica Acta, vol. 44, pp. 1329-1339, 1998.